Mechanism and Energetics for Complexation of ^{90}Y with 1,4,7,10-Tetraazacyclododecane-1,4,7,10-tetraacetic Acid (DOTA), a Model for Cancer Radioimmunotherapy

Yun Hee Jang,[†] Mario Blanco,[†] Siddharth Dasgupta,[†] David A. Keire,[‡] John E. Shively,[‡] and William A. Goddard III*,[†]

Contribution from the Materials and Process Simulation Center, Beckman Institute (139-74), California Institute of Technology, Pasadena, California 91125, and The Beckman Research Institute of the City of Hope, 1450 East Duarte Road, Duarte, California

Received October 21, 1998. Revised Manuscript Received March 30, 1999

Abstract: A promising cancer therapy involves the use of the macrocyclic polyaminoacetate DOTA (1,4,7,10-tetraazacyclododecane-1,4,7,10-tetraacetic acid) attached to a tumor-targeting antibody complexed with the β emitter $^{90}Y^{3+}$. However, incorporation of the ^{90}Y into the DOTA conjugate is too slow. To identify the origins of this problem, we used ab initio quantum chemistry methods (B3LYP/LACVP* and HF/LACVP*) to predict structures and energetics. We find that the initial complex $YH_2(DOTA)^+$ is 4-coordinate (the four equivalent carboxylate oxygens), which transforms to YH(DOTA) (5-coordinate with one ring N and four carboxylate oxygens), and finally to $Y(DOTA)^-$, which is 8-coordinate (four oxygens and four nitrogens). The rate-determining step is the conversion of YH(DOTA) to $Y(DOTA)^-$, which we calculate to have an activation free energy (aqueous phase) of 8.4 kcal/mol, in agreement with experimental results (8.1−9.3 kcal/mol) for various metals to DOTA [Kumar, K.; Tweedle, M. F. *Inorg. Chem.* **1993**, *32*, 4193−4199; Wu, S. L.; Horrocks, W. D., Jr. *Inorg. Chem.* **1995**, *34*, 3724−3732]. On the basis of this mechanism we propose a modified chelate, DO3AlPr, which we calculate to have a much faster rate of incorporation.

1. Introduction

Tumor-targeting with radioisotope-labeled antibodies[1] is being used for (a) cancer radioimmunotherapy (with $^{90}Y^{3+}$ as a β-emitter), (b) cancer diagnosis (with $^{111}In^{3+}$ and $^{67}Ga^{3+}$ as γ-emitters or with $^{64}Cu^{2+}$ as a positron-emitter), and (c) in vivo magnetic resonance imaging (MRI) (with Gd^{3+} as a paramagnetic contrast agent).[2]

Central to the success of such approaches is the development of bifunctional chelating agents[1] containing both a reactive functionality for covalent attachment to the antibody and a strong cation-binding group capable of forming rapidly and selectively an inert complex with radionuclides (Scheme 1).[3,4]

To reduce radiation damage to normal organs and tissues, radioimmuotherapy requires that the radionuclide form a stable and inert complex of the chelant−antibody conjugate under physiological conditions.[1,4] Otherwise, "the build-up of significant amounts of $^{90}Y^{3+}$ in the bone after the premature release from the complex could lead to myelosuppression (depletion of the immune cell population) due to irradiation of the proximate bone-marrow, with a dramatically increased risk of infection".[1] Initial results with derivatives of EDTA (ethylenediaminetetraacetatic acid; Scheme 2a) and DTPA (diethylenetriaminepentaacetic acid; Scheme 2b) were disappointing due to the instability of their complexes in vivo.[1,4]

Scheme 1. Schematic Drawing Showing the Basics of Radioimmunotherapy[a]

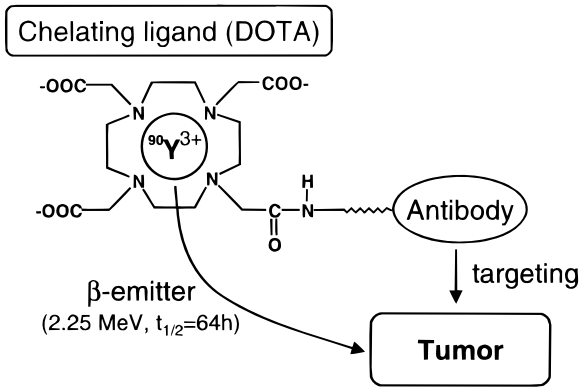

[a] The tumor-targeting antibody is labeled with radionuclide such as $^{90}Y^{3+}$ by using a bifunctional chelating agent such as DOTA.

Derivatives of DOTA (Scheme 2c) constitute a promising class of chelating agents for radiotherapy because they form extremely stable and inert complexes with a wide variety of metal cations.[4−9] For example, less than 0.5% of Y dissociated

* To whom correspondence should be addressed (wag@wag.caltech.edu).
† California Institute of Technology.
‡ The Beckman Research Institute of the City of Hope.

(1) Parker, D. *Chem. Soc. Rev.* **1990**, *19*, 271−291.
(2) Lauffer, R. B. *Chem. Rev.* **1987**, *87*, 901−927.
(3) Lewis, M. R.; Raubitschek, A.; Shively, J. E. *Bioconjugate Chem.* **1994**, *5*, 565−576.
(4) Broan, C. J.; Cox, J. P. L.; Craig, A. S.; Kataky, R.; Parker, D.; Harrison, A.; Randall, A. M.; Ferguson, G. *J. Chem. Soc., Perkin Trans. 2* **1991**, 87−99.
(5) Wang, X. Y.; Jin, T. Z.; Comblin, V.; Lopezmut, A.; Merciny, E.; Desreux, J. F. *Inorg. Chem.* **1992**, *31*, 1095−1099.
(6) Clarke, E. T.; Martell, A. E. *Inorg. Chim. Acta* **1991**, *190*, 37−46.
(7) Kodama, M.; Koike, T.; Mahatma, A. B.; Kimura, E. *Inorg. Chem.* **1991**, *30*, 1270−1273.
(8) Loncin, M. F.; Desreux, J. F.; Merciny, E. *Inorg. Chem.* **1986**, *25*, 2646−2648.
(9) Desreux, J. F. *Inorg. Chem.* **1980**, *19*, 1319−1324.

10.1021/ja983706q CCC: $18.00
Published on Web 06/22/1999

Scheme 2

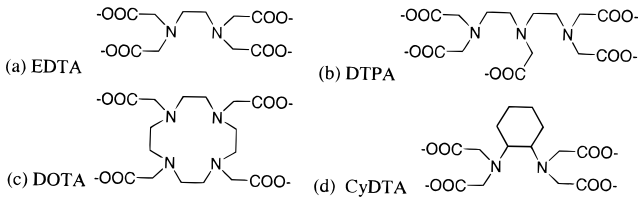

Scheme 3. Kinetics of the Formation of Complex between DOTA (L) and Metal Ion (M)

$$M^{3+} + H_2L^{2-} \xleftrightarrow{fast} [M(H^*{}_2L)^+] \text{ or } [M(H^*L) + H^+]$$

Type I (intermediate)

$$\xrightarrow{slow} ML^- + 2H^+$$

Type II (final complex)

from a DOTA-type ligand over 18 days in serum (pH 7.4, 37 °C).[1,10] Similarly, the $^{90}Y-DOTA$ complex showed no change during 72 h at pH 5.5 even with a 500-fold excess of DTPA.[4] In addition, $Gd(DOTA)^-$ (a useful contrast agent in the nuclear magnetic resonance imaging) has a half-life of ~85 days at pH 2 and more than 200 days at pH 5.[5] These complexes are remarkably rigid and nonlabile, an unusual property not exhibited by the complexes of acyclic analogues such as EDTA or DTPA.[8] The tetraaza macrocycle of DOTA acts as a frame to constrain its eight donor atoms (four tertiary nitrogen atoms and four carboxylic groups) into a nearly spherical arrangement (eight vertices of a square antiprism). Here the tetraaza ring adopts the quadrangular [3333] conformation,[8,9] which is the most stable conformation of cyclododecane.[11]

However, despite the stability and inertness of their complexes with metal ions, DOTA-like compounds have a potentially serious limitation for these radioimmunotherapy applications because the formation of metal−DOTA complexes is too slow.[3,7,9,12] Since the radioisotope is short-lived (a half-life of ^{90}Y of 60 h), it is essential that the chemical processing steps be very fast. Unfortunately, the formation rate for the Y−DOTA complex is nearly 1600 times slower than that for Y−DTPA.[7] "Slow complex formation presents a challenge to achieving a good radiolabeling yield in a short time."[3]

Various experimental results[5,13−16] suggested the mechanism in Scheme 3 for the formation of the $M(DOTA)^-$ complex (M = Y or other trivalent metal ions). In the pH range 3−8, DOTA is present in the forms $H_2(DOTA)^{2-}$, $H_3(DOTA)^-$, and $H_4(DOTA)$,[1,6,16] and in the pH range 6−7, DOTA exists primarily (>90%) as $H_2(DOTA)^{2-}$.[6,15] (The protonation constants (pK_a values) of DOTA are 11.14, 9.69, 4.85, and 3.95 at 25.0 °C with 0.100 M KCl.[6]) The formation of $M(DOTA)^-$ complexes proceeds via two steps: (a) first, a fast formation of a stable intermediate (type I), and (b) second, a slow conversion into the final complex (type II) with the release of a proton from its precursor MH(DOTA). The rate of formation of the type II complex is proportional to $[H^+]^{-1}$. The rate-determining step is the base-catalyzed type I → II transformation.[5,12−18]

However, the details about **how** the deprotonation occurs from the type I intermediate are not known. There is controversy even in the degree of protonation of the intermediate [$MH_2(DOTA)^+$ versus MH(DOTA)] and the conformation of the type I complex (coordination just by four carboxylates or coordination by carboxylates and a ring nitrogen).[5,12−17]

Wu and Horrocks,[15] Burai et al.,[12] Brucher et al.,[13] and Toth et al.[16] suggested $MH_2(DOTA)^+$ as the long-lived type I complex of DOTA with Eu^{3+}, Ce^{3+}, and other lanthanides. It has protons at two ring nitrogen atoms trans to each other. It does **not** have the M^{3+} in the cage determined by the four ring nitrogen and four acetate oxygen atoms; rather it is coordinated only by four acetate oxygen atoms on the side away from the plane of the macrocyclic ring because of the repulsion between M^{3+} and the ring protons. [The calculation (Figure 2a below) shows the same characteristics for $MH_2(DOTA)^+$.] This $MH_2(DOTA)^+$ is in equilibrium with MH(DOTA) and these two species have similar (or identical) structures.[12,15] [The calculation (Figure 2a,b) shows different structures for $MH_2(DOTA)^+$ and MH(DOTA).] In the final rate-determining step, the metal ion (M^{3+}) enters into the fully coordinated type II complex simultaneously with the slow deprotonation of the MH(DOTA) intermediate.[12,13,15,16] [This is consistent with the calculation below.]

On the other hand, Kumar and Tweedle,[17] Wang et al.,[5] and Kasprzyk and Wilkins[14] proposed that the type I intermediate leading to the final complex is the singly protonated MH(L) (L = DOTA or triacetate derivatives of DOTA) with the proton on a ring nitrogen. They suggested that this intermediate has M^{3+} coordinated to at least one nitrogen in addition to the three carboxylate oxygens. [This is consistent with the calculation (Figure 2b below).] In addition, they hypothesized that the stable protonated form of the chelate is ML(H) with the proton on a carboxylate oxygen. (The stability constants of ML(H) complexes are 2−7 orders of magnitude higher than the stability constants of MH(L) intermediates.) This model is essentially the same as that suggested by Nyssen and Margerum for the Ln−CyDTA complex[19] (CyDTA = *trans*-1,2-diaminocyclohexane-*N*,*N*,*N*′,*N*′-tetraacetic acid; Scheme 2d). [We find below that the rate-determining step for the type I → II reaction is the migration of the proton from a ring nitrogen to its carboxylate oxygen (Figure 6).]

To design more effective and selective bifunctional chelating agents that would transform to type II more rapidly, we focused our studies on the mechanism and energetics of the type I → II reaction. To investigate the structural change of DOTA in the course of complexation with Y^{3+}, we performed ab initio quantum-mechanical calculations[20] including solvation by water (using the Poisson−Boltzmann continuum solvation model).[21−23] Although several theoretical studies on the Gd complex of

(10) Moi, M. K.; Meares, C. F.; Denardo, S. J. *J. Am. Chem. Soc.* **1988**, *110*, 6266−6267.
(11) Anet, F. A. L.; Rawdah, T. N. *J. Am. Chem. Soc.* **1978**, *100*, 7166−7171.
(12) Burai, L.; Fabian, I.; Kiraly, R.; Szilagyi, E.; Brucher, E. *J. Chem. Soc., Dalton Trans.* **1998**, 243−248.
(13) Brucher, E.; Laurenczy, G.; Makra, Z. *Inorg. Chim. Acta* **1987**, *139*, 141−142.
(14) Kasprzyk, S. P.; Wilkins, R. G. *Inorg. Chem.* **1982**, *21*, 3349−3352.
(15) Wu, S. L.; Horrocks, W. D., Jr. *Inorg. Chem.* **1995**, *34*, 3724−3732.
(16) Toth, E.; Brucher, E.; Lazar, I.; Toth, I. *Inorg. Chem.* **1994**, *33*, 4070−4076.
(17) Kumar, K.; Tweedle, M. F. *Inorg. Chem.* **1993**, *32*, 4193−4199.
(18) Kumar, K.; Jin, T. Z.; Wang, X. Y.; Desreux, J. F.; Tweedle, M. F. *Inorg. Chem.* **1994**, *33*, 3823−3829.
(19) Nyssen, G. A.; Margerum, D. W. *Inorg. Chem.* **1970**, *9*, 1814−1820.
(20) *Jaguar 3.5*; Schrodinger Inc.: Portland, OR, 1998.
(21) Tannor, D. J.; Marten, B.; Murphy, R.; Friesner, R. A.; Sitkoff, D.; Nicholls, A.; Ringnalda, M.; Goddard, W. A., III; Honig, B. *J. Am. Chem. Soc.* **1994**, *116*, 11875−11882.
(22) Marten, B.; Kim, K.; Cortis, C.; Friesner, R. A.; Murphy, R. B.; Ringnalda, M. N.; Sitkoff, D.; Honig, B. *J. Phys. Chem.* **1996**, *100*, 11775−11788.
(23) Honig, B.; Nicholls, A. *Science* **1995**, *268*, 1144−1149.

DOTA- and DTPA-type compounds[24−27] have been reported, they focused on the stabilities of the final complexes rather than the energetics involved in complex formation. In this work we concentrate on the formation of the Y complex with the unmodified DOTA, without any linkage to antibodies.

Section 2 describes the calculational details while Section 3 presents the results on the two conformations (*M* and *m*) of $Y(DOTA)^-$. Section 4 discusses the structures of $YH_n(DOTA)_{n-1}$ while Section 5 examines the mechanism of proton removal from YH(DOTA) (the rate-determining step). Finally, Section 6 proposes a DOTA modification for which incorporation of Y^{3+} should be much faster than that for DOTA.

2. Calculational Details

2.1. Quantum Chemistry. All calculations were performed with the Jaguar v3.5 quantum chemistry software.[20] Geometries were optimized at the HF level with the LACVP* basis set [6-31G* for C, O, N, and H]. For Y, the effective core potentials (ECP) of Hay and Wadt[28] were used to replace the core electrons ($1s^22s^22p^63s^23p^63d^{10}$), leaving only the outermost 11 electrons ($4s^24p^65s^24d^1$) to be calculated explicitly. This leads to 466 basis functions for $YH_2(DOTA)^+$. The calculated stationary points were characterized by calculating the vibration frequencies with the Hessian obtained during the geometry optimization. We determined that every frequency is real at the minima with one and only one imaginary frequency for each saddle point (transition state).

2.2. Solvation. The solvation in water was described with use of the continuum-solvation approach[21−23] by solving the Poisson−Boltzmann (PB) equation numerically.[29] In this approach, the solute is described as a low-dielectric cavity ($\epsilon = 1$) immersed in a high-dielectric continuum of solvent ($\epsilon = 80$ for water). The solute/solvent boundary is described by the surface of closest approach as a sphere of radius 1.4 Å (probe radius for water) is rolled over the van der Waals (vdW) envelope of the solute. The charge distribution of the solute is represented by a set of atom-centered point charges, which are determined by fitting to the electrostatic potential calculated from the wave function. A gas-phase calculation is carried out first to obtain these electrostatic-potential fitted (ESP) charges. On the basis of these charges, the PB equation is solved to obtain the reaction field of the solvent (as a set of polarization charges located on the solute/solvent boundary surface). The Fock−Hamiltonian for the HF calculation is then modified to include the solute−solvent interaction due to the reaction field. This is solved to obtain a new wave function and a new set of atom-centered ESP charges. This process is repeated self-consistently until convergence is reached (to 0.1 kcal/mol in the solvation energy). This constitutes the electrostatic or "polar" contribution to the solvation energy.

An additional "nonpolar" contribution due to creation of a solute cavity in the solvent is accounted for by a term proportional to the solvent-accessible surface area of the solute.[21,22]

The atomic radii used to build the vdW envelope of the solute were determined as follows: For Y^{3+}, we calculated that a Y radius of 1.807 Å leads to a solvation energy of −826.1 kcal/mol in water, in good agreement with the experimental free energy of solvation of −825[30] to −826.2[31] kcal/mol. For DOTA, the radii of 1.9 Å for C, 1.6 Å for O and N, and 1.15 Å for H were based on earlier studies.[21−23]

In addition to the eight ligands from DOTA, we expect[32] that the $Y(DOTA)^-$ complex would have one water molecule also coordinated to Y^{3+}, leading to 9-coordinate Y^{3+}. The $YH_2(DOTA)^+$ and YH(DOTA) complexes would also have several water molecules coordinated in their inner shells to satisfy the 9-coordination around Y^{3+}.[15] We do not include these water molecules explicitly in the calculations, because it is assumed that the effect of this water molecule is taken into account implicitly by the continuum solvation model. However, there can be significant change in the complexation energetics when these water molecules are taken into account explicitly, especially if the stripping-off of these water molecules is important for Y^{3+} to move toward the inside of the DOTA cage.[33] The number of water molecules coordinated to Y^{3+} in each conformer of $YH_n(DOTA)^{n-1}$ ($n = 0$, 1, and 2) and their effect on the complexation energetics will be investigated later.

3. Isomers of $Y(DOTA)^-$

It is well-known that two isomers of $M(DOTA)^-$ are observed in solution and in the crystal.[9,34−38] The major isomer *M* has the regular antiprism geometry and the minor isomer *m* has the inverted antiprism geometry (both C_4 symmetry). These differ in the orientation (helicity) of the carboxylate arms but have the same conformation of the tetraaza cycles,[34,35,37,38] as seen in Figure 1. The crystal structure of $Y(DOTA)^-$ corresponds to the *M* isomer,[32,39] but the crystal structure of $Y(DO3TA)^-$ [DO3TA=10-(2-hydroxypropyl)-1,4,7,10-tetraazacyclododecane-1,4,7-triacetic acid], which is similar to that of $Y(DOTA)^-$, shows both *M* and *m* isomers in one crystal.[40] The energy difference between *M* and *m* is a few kilocalories per mole, but the barrier of interconversion from *M* to *m* is quite high; for example, in the case of $Yb(DOTA)^-$ complex, *M* is more stable than *m* by 4.3 kcal/mol, but the experimental barrier of interconversion from *M* to *m* is 22 kcal/mol.[35]

Our calculations indicate that gas-phase *M* is more stable by 1.6 kcal/mol than *m*, but that aqueous phase *m* is more stable than *M* by 0.88 kcal/mol. This result might seem to contradict the experimental observation of the *M* isomer in the crystal structure.[32,39] There can be an effect of molecular contact and packing on the relative stability of *M* and *m*, which is not included in the current calculation. Moreover, the crystal phase corresponds to a low-dielectric medium that is closer to the gas phase than to the aqueous phase. Thus, our gas-phase calculation is consistent with the crystal structure experiment. Unfortunately, for Y(DOTA) there is no report on which species is dominant in the solution phase. Our calculations indicate that in aqueous solution at 298 K, about 77% of the Y(DOTA) should be the *m* conformation, assuming that $\Delta G(M \rightarrow m)$ is equal to $\Delta E(M \rightarrow m)$. Thus, we focused our calculations on the *m* isomer. [In Section 4.1 we report calculations for both isomers to find that the structural changes in complex formation are essentially the same for both conformers.]

(24) Cosentino, U.; Moro, G.; Pitea, D.; Villa, A.; Fantucci, P. C.; Maiocchi, A.; Uggeri, F. *J. Phys. Chem. A* **1998**, *102*, 4606−4614.
(25) Reichert, D. E.; Hancock, R. D.; Welch, M. J. *Inorg. Chem.* **1996**, *35*, 7013−7020.
(26) Fossheim, R.; Dahl, S. G. *Acta Chem. Scand.* **1990**, *44*, 698−706.
(27) Fossheim, R.; Dugstad, H.; Dahl, S. G. *J. Med. Chem.* **1991**, *34*, 819−826.
(28) Hay, P. J.; Wadt, W. R. *J. Chem. Phys.* **1985**, *82*, 299−310.
(29) Nicholls, A.; Honig, B. *J. Comput. Chem.* **1991**, *12*, 435−445.
(30) Marcus, Y. *J. Chem. Soc., Faraday Trans.* **1991**, *87*, 2995−2999.
(31) Marcus, Y. *Ion Solvation*; Wiley: New York, 1985; p 107.
(32) Chang, C. A.; Francesconi, L. C.; Malley, M. F.; Kumar, K.; Gougoutas, J. Z.; Tweedle, M. F.; Lee, D. W.; Wilson, L. J. *Inorg. Chem.* **1993**, *32*, 3501−3508.
(33) Wu, S. L.; Johnson, K. A.; Horrocks, W. D., Jr. *Inorg. Chem.* **1997**, *36*, 1884−1889.
(34) Aime, S.; Botta, M.; Ermondi, G. *Inorg. Chem.* **1992**, *31*, 4291−4299.
(35) Jacques, V.; Desreux, J. F. *Inorg. Chem.* **1994**, *33*, 4048−4053.
(36) Marques, M. P. M.; Geraldes, C. F. G. C.; Sherry, A. D.; Merbach, A. E.; Powell, H.; Pubanz, D.; Aime, S.; Botta, M. *J. Alloys Compd.* **1995**, *225*, 303−307.
(37) Aime, S.; Botta, M.; Fasano, M.; Marques, M. P. M.; Geraldes, C. F. G. C.; Pubanz, D.; Merbach, A. E. *Inorg. Chem.* **1997**, *36*, 2059−2068.
(38) Lincoln, S. F. *Coord. Chem. Rev.* **1997**, *166*, 255−289.
(39) Parker, D.; Pulukkody, K.; Smith, F. C.; Batsanov, A.; Howard, J. A. K. *J. Chem. Soc., Dalton Trans.* **1994**, 689−693.
(40) Kumar, K.; Chang, C. A.; Francesconi, L. C.; Dischino, D. D.; Malley, M. F.; Gougoutas, J. Z.; Tweedle, M. F. *Inorg. Chem.* **1994**, *33*, 3567−3575.

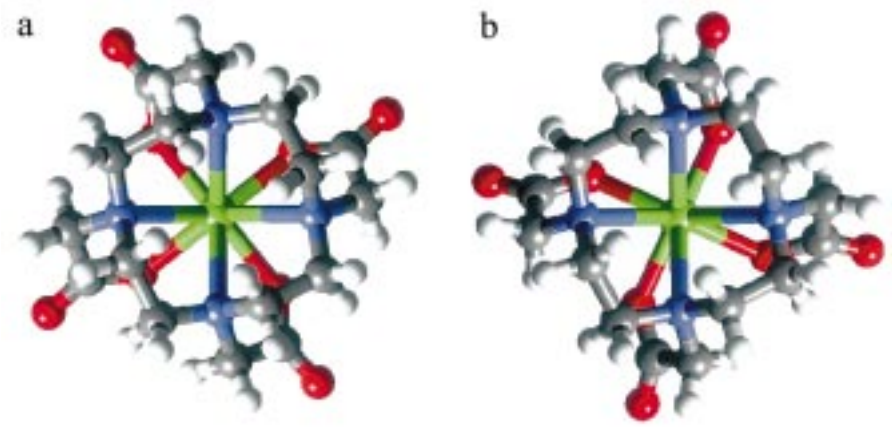

Figure 1. Top view of two Y(DOTA)$^-$ isomers: (a) major isomer (*M*) and (b) minor isomer (*m*). The root-mean-square deviation between the ring structures of *M* and *m* is only 0.03 Å. Color key: green, Y; blue, N; red, O; gray, C; and white, H. The water coordinated at the ninth coordination position is not shown here.

Table 1. Geometric and Energy Parameters of $YH_n(DOTA)^{n-1}$ (n = 2, 1, 0) in the Gas Phase[a]

	(a) $YH_2(DOTA)^+$ calcd		(b) YH(DOTA) calcd		(c) $Y(DOTA)^-$ calcd		(d) $Y(DOTA)^- - H_2O$ X-ray[b]
	M	*m*	*M*	*m*	*M*	*m*	*M*
O−Y (Å)	**2.169**	**2.200**	**2.271**	**2.278**	**2.272**	**2.272**	**2.273**
	2.171	**2.205**	**2.182**	**2.176**	**2.272**	**2.274**	**2.315**
	2.140	**2.149**	**2.249**	**2.208**	**2.272**	**2.274**	**2.274**
	2.146	**2.175**	**2.175**	**2.183**	**2.273**	**2.274**	**2.322**
N−Y (Å)	3.928	4.069	3.758	3.855	**2.724**	**2.755**	**2.777**
	3.937	4.013	**2.746**	**2.742**	**2.724**	**2.756**	**2.780**
	3.887	4.011	2.941	3.021	**2.725**	**2.755**	**2.744**
	3.898	4.154	3.195	3.357	**2.727**	**2.757**	**2.805**
H−Y (Å)	3.037	3.190	2.755	2.864			
	3.044	3.142					
O−H (Å)	2.348	2.168	1.863	1.855			
	2.363	2.259					
N−H (Å)	1.007	1.011	1.009	1.013			
	1.007	1.010					
O−Y−O (deg)[c]	140.2(+)	131.2(+)	169.88(−)	174.96(+)	144.50(−)	141.69(−)	143.1(−)
	139.8(+)	125.1(+)	153.10(−)	154.81(−)	144.55(−)	141.89(−)	144.8(−)
energy ($m - M$) (kcal/mol)							
gas phase					0.0	1.6	
solvated					0.0	−0.88	

[a] Bonded ligands are shown in bold face. [b] Reference 39. [c] (+)/(−) indicates that Y is outside/inside the cage, respectively.

4. Structure of $YH_n(DOTA)^{n-1}$ (n = 2, 1, 0)

4.1. Crab-like Conformations. We optimized the structure of $YH_2(DOTA)^+$, starting from the crab-like 4-coordinate conformation in which the protons are located on two trans ring nitrogens and the ion Y^{3+} is coordinated by four carboxylate groups, as suggested by many experiments.[5,12−16] Then, the proton from one ring nitrogen was removed and the structure of YH(DOTA) reoptimized to determine the change in conformation after deprotonation from $YH_2(DOTA)^+$. Finally, the other proton was removed and the structure of $Y(DOTA)^-$ reoptimized. Because two isomers of $M(DOTA)^-$ are observed in solution and in the crystal,[9,34,35,37,38] we did the same kind of calculations for both isomers. [As the starting conformations of $YH_2(DOTA)^+$ for the *M* and *m* isomers, we assumed the same [3333] geometry[8,9,11] for the tetraaza ring, but two different orientations were chosen for the carboxylate arms to represent two isomers[34,35,38] (see Figure 1).] We found that the *M* and *m* isomers show essentially the same structural changes after deprotonation (see Table 1).

In the doubly protonated complex $YH_2(DOTA)^+$, Y^{3+} is located outside the cage composed of carboxylate oxygens and ring nitrogens (O−Y = 2.1−2.2 Å, N−Y = 3.8−4.2 Å) and is coordinated only by carboxylate oxygens (see Table 1a and Figure 2a).

Upon removal of one proton from the ring nitrogen to form YH(DOTA), the Y^{3+} moves toward the ring to become coordinated to four carboxylate oxygens and the one ring nitrogen trans to the protonated nitrogen. (Table 1b and Figure 2b show that one N−Y distance decreased to 2.74 Å.) In this structure Y^{3+} is located in the oxygen plane of the ligand and the nitrogen plane is distorted so that one nitrogen is also coordinated to Y^{3+}. This is exactly the structure suggested by Kumar and Tweedle.[17]

With removal of the last proton to form $Y(DOTA)^-$, the Y^{3+} moves farther into the cage, becoming octadentate coordinated (four O−Y at 2.27 Å, four N−Y at 2.72−2.76 Å; see Table 1c and Figure 2c). This structure is essentially the same as in the X-ray structure of $Y(DOTA)^-$ (O−Y = 2.27 to 2.32 Å and N−Y = 2.74−2.80 Å)[32,39] (see Table 1d). The root-mean-square (rms) deviation between the calculated and experimental structures of $Y(DOTA)^-$ is only 0.1 Å.

These results indicate that repulsion between Y^{3+} and the nitrogen protons plays an important role in determining the

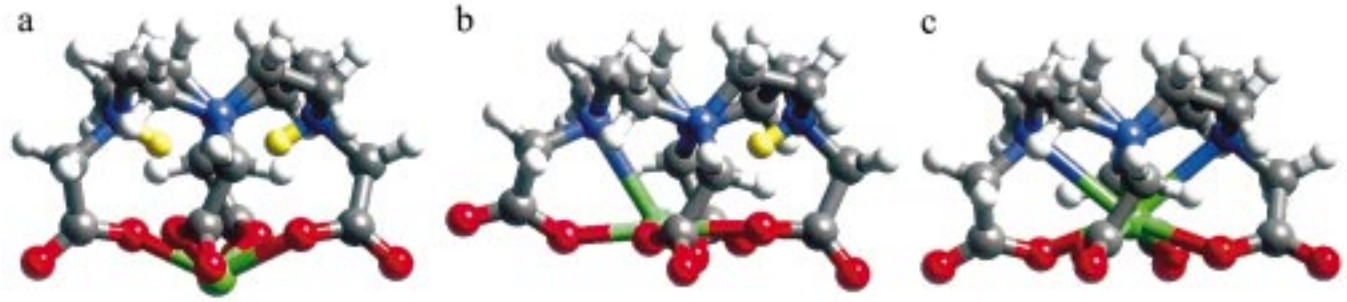

Figure 2. (a) $YH_2(DOTA)^+$ started from the experimentally suggested 4-coordinate structure, (b) YH(DOTA) started from $YH_2(DOTA)^+$ with one nitrogen proton removed (it is 5-coordinate), and (c) $Y(DOTA)^-$ started from YH(DOTA) with one more nitrogen proton removed (it is 8-coordinate). Color key: green, Y; blue, N; red, O; gray, C; white, H; and yellow, H attached to the ring N. The water molecules coordinated in the inner coordination shell are not shown here.

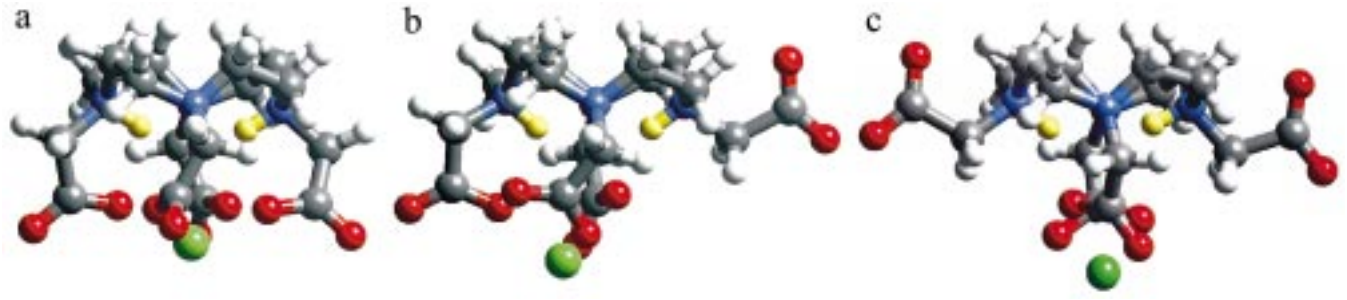

Figure 3. Conformational isomers of $YH_2(DOTA)^+$: (a) 4-coordinate conformer, (b) 3-coordinate conformer, and (c) 2-coordinate conformer. Color key: green, Y; blue, N; red, O; gray, C; white, H; and yellow, H attached to the ring N. Each coordination number refers just to the coordination by DOTA. The water coordination in the inner coordination shell is not counted. The water molecules coordinated in the inner coordination shell are not shown here.

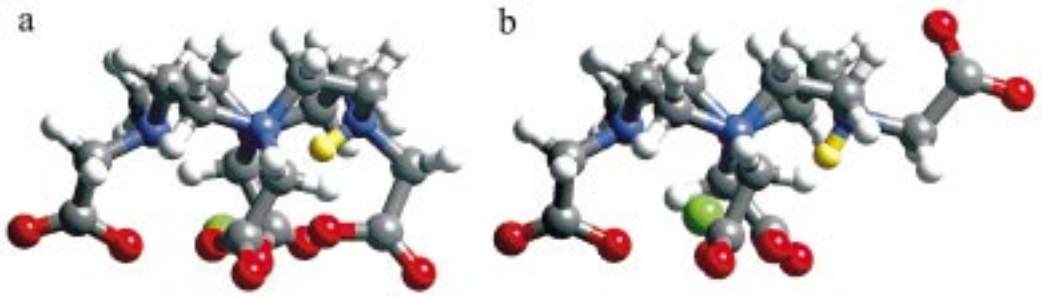

Figure 4. Conformational isomers of YH(DOTA): (a) 4-coordinate conformer and (b) 3-coordinate conformer. Color key: green, Y; blue, N; red, O; gray, C; white, H; and yellow, H attached to the ring N. Each coordination number refers just to the coordination by DOTA. The water coordination in the inner coordination shell is not counted. The water molecules coordinated in the inner coordination shell are not shown here.

structure of the complex (as also suggested from other studies[5,16,17]). Upon deprotonation of YH(DOTA), Y^{3+} simultaneously enters into the cage from the outside. There is little change in the ring conformation after deprotonation and recoordination around the Y^{3+}. (The rms deviation between the ring conformations of these three species is less than 0.5 Å.) This indicates that upon formation of the crab-like conformation of DOTA (which is favorable for forming a Y complex) and removal of the protons on the nitrogens, it will form a stable Y complex spontaneously without any additional cost due to conformational change. Thus, the deprotonation is the rate-determining step followed by fast rearrangement, in agreement with the view from some experiments.[12,13,15,17]

4.2. Does DOTA Prefer the Crab-like Conformation? Comparison with Extended Conformations. The above calculations started with crab-like 4-coordinate conformations for $YH_2(DOTA)^+$ and YH(DOTA), as suggested from previous works.[5,12−16] To determine whether these crab-like 4-coordinate structures (shown in Figures 2, 3a, and 4a) are really more stable than other possible conformations, we calculated the structures and energies (both gas-phase and aqueous phase) for the more extended 2- or 3-coordinate structures shown in Figures 3b, 3c, and 4b).

These results (Table 2) indicate that the crab-like 4-coordinate conformation is significantly more stable than the others (by 17−43 kcal/mol), even in the aqueous phase (where more extended conformation might be expected to be preferred).

5. Mechanism of Proton Removal [$YH(DOTA) \rightarrow Y(DOTA)^- + H^+$]

5.1. Energy Barrier for Proton Transfer from NH to COO. In the most stable crab-like 4-coordinate conformation of $YH_2(DOTA)^+$ and YH(DOTA), the proton on the ring nitrogen is located inside the cage and is not accessible to outside base (OH^- or H_2O). This is shown in Figure 5. To expose the proton to the outside base, one might expect that this structure would open up to form the 3- or 2-coordinate conformations. However, the energy cost is 17 kcal/mol for $YH_2(DOTA)^+$ and 22 kcal/mol for YH(DOTA) (see Table 2). This high energy

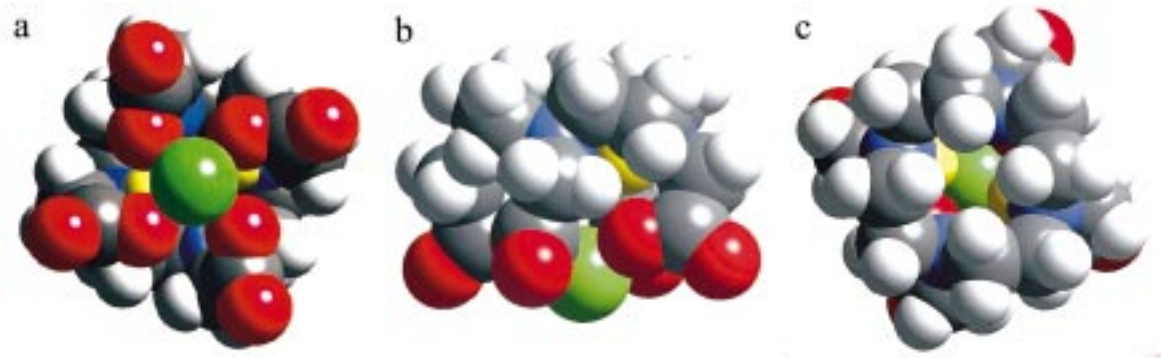

Figure 5. Space-filling representation of the crab-like 4-coordinate conformation of YH(DOTA) viewed from the (a) bottom, (b) side, and (c) top. Color key: green, Y; blue, N; red, O; gray, C; white, H; and yellow, H attached to ring N. The water molecules coordinated in the inner coordination shell are not shown here.

Table 2. Energies of Various Conformations of $YH_2(DOTA)^+$ and YH(DOTA)

		$YH_2(DOTA)^+$			YH(DOTA)	
rel energy (kcal/mol)		**4-coord**	3-coord	2-coord	**4-coord**	3-coord
gas phase	HF	0	39.9	109.8	0	27.4
	B3LYP//HF	0	36.8	104.8	0	22.1
(solvation	HF	(−148.1)	(−170.2)	(−220.0)	(−86.2)	(−88.2)
energy)	B3LYP//HF	(−126.4)	(−146.7)	(−188.5)	(−68.3)	(−68.7)
aq phase	HF	0	17.8	37.9	0	25.4
	B3LYP//HF	**0**	**16.6**	**42.7**	**0**	**21.6**

barrier for exposing the proton is consistent with the rate-determining step being removal of the proton, and explains the unusually slow formation of $Y(DOTA)^-$ complex and the existence of the unusually stable intermediates.[5,12−16]

How the proton is removed from these intermediates and the energy barrier of this deprotonation process remains a question. Two possible pathways for deprotonating these intermediates have been proposed: (1) insertion of water or hydroxide into the cage, as suggested by Toth et al.,[16] and (2) nitrogen inversion, as suggested by Kumar and Tweedle.[17]

However, the structure in Figure 5 shows that the proton is not exposed to solvent. Thus, the plausibility of pathway 1 depends on the conformational flexibility of the intermediates. $YH_2(DOTA)^+$ was suggested[15,16] to have a labile Y−acetate bond and to show fast exchange of Y^{3+} between $YH_2(DOTA)^+$ and Y^{3+}(aq). In this case the nitrogen proton of the doubly protonated intermediate can be exposed to outside base. However, in YH(DOTA) the Y^{3+} is coordinated to one ring nitrogen as well as four carboxylate groups, leading to a structure expected to be more rigid with insufficient flexibility to expose the ring proton to outside base. Thus, pathway 1 might work for $YH_2(DOTA)^+$ but not for YH(DOTA).

Pathway 2 is not plausible because quaternary amines (the protonated amine) have large nitrogen inversion barriers.[41−44]

On the basis of our calculations, we find an alternative pathway for deprotonation that is favorable for YH(DOTA): (3) proton transfer from the ring nitrogen to the carboxylate oxygen, making the proton more accessible to outside base.

In the optimized structure of YH(DOTA), we found that the carboxylate oxygen is located very close to the proton attached to the ring nitrogen (the distance between the proton and the oxygen [(N)H···O] is 1.8 Å, the distance between the protonated nitrogen and the oxygen [N(H)···O] is 2.5 Å, and the angle from the nitrogen through the proton to the oxygen [N−H···O] is 124°), which is a very favorable situation for proton transfer between N and O. The proton transfer from ring nitrogen to carboxylate oxygen [pathway 3] is the reverse of the proposed acid-catalyzed dissociation pathway of $Y(DOTA)^-$: (a) protonation on carboxylate site, (b) proton transfer to ring nitrogen, followed by (c) repulsion between Y^{3+} and proton to ease the dissociation.[5,14,16,18]

We calculated the optimized structures of the transition state and the product of the proton transfer from the ring nitrogen in YH(DOTA) to the carboxylate oxygen [denoted as Y(DOTA)−H] and calculated the energy barrier of this process (see Figure 6 and Table 3). These results show that, as the proton is transferred from the ring nitrogen to the carboxylate oxygen, Y^{3+} goes toward the ring in the spontaneous and concerted manner to form the octadentate coordination complex (see Figure 6). The proton attached to the carboxylate group in Figure 6c will be removed very fast by outside base to form the final $Y(DOTA)^-$ complex. The energy barrier (i.e., the energy difference between the reactant and the transition state) was calculated (at the B3LYP//HF level) to be 2.0 kcal/mol in the gas phase and 12.2 kcal/mol in the aqueous phase. This is lower than the energy cost needed to expose the ring proton by changing the conformation (21.6 kcal/mol; see Section 4.2). Thus, we conclude that pathway 3 is strongly favored over pathways 1 and 2. Once the proton transfer occurs to form Y(DOTA−H) (at moderate energy cost), the formation of the final $Y(DOTA)^-$ complex is quite favorable because there is little conformational change required in the DOTA.

The barrier is 2 kcal/mol in the gas phase and 12.2 kcal/mol in the aqueous phase, indicating that solvation leads to a significant destabilization of the transition state. We considered two likely origins of this.

(a) The first is the desolvation of Y^{3+} after it moves slightly toward the cage. Since the solvation energy of Y^{3+} is huge (>800 kcal/mol), this slight desolvation might lead to a significant energy change. We tested this by comparing the energetics obtained with different radii of yttrium used in the solvation calculation (1.807 and 1.673 Å). We found that the energy barrier was the same, showing a negligible desolvation of Y^{3+} from the reactant to the transition state. Thus, we exclude this explanation.

(b) A second plausible origin is that the solvation of the charge-delocalized transition state (such as for N···H···O) is less favorable than the charge-localized reactant ($NH^+ + O^-$). We tested this by doing calculations on *N*-dimethylglycine

(41) Pitner, T. P.; Martin, R. B. *J. Am. Chem. Soc.* **1971**, *93*, 4401−4405.
(42) Wilkins, R. G. *The Study of Kinetics and Mechanism of Reactions of Transition Metal Complexes*; Allyn & Bacon: Boston, 1974.
(43) Buckingham, D. A.; Clark, C. R.; Rogers, A. J. *J. Am. Chem. Soc.* **1997**, *119*, 4050−4058.
(44) Delpuech, J. J. *Cyclic Organonitrogen Stereodynamics*; VCH: New York, 1992.

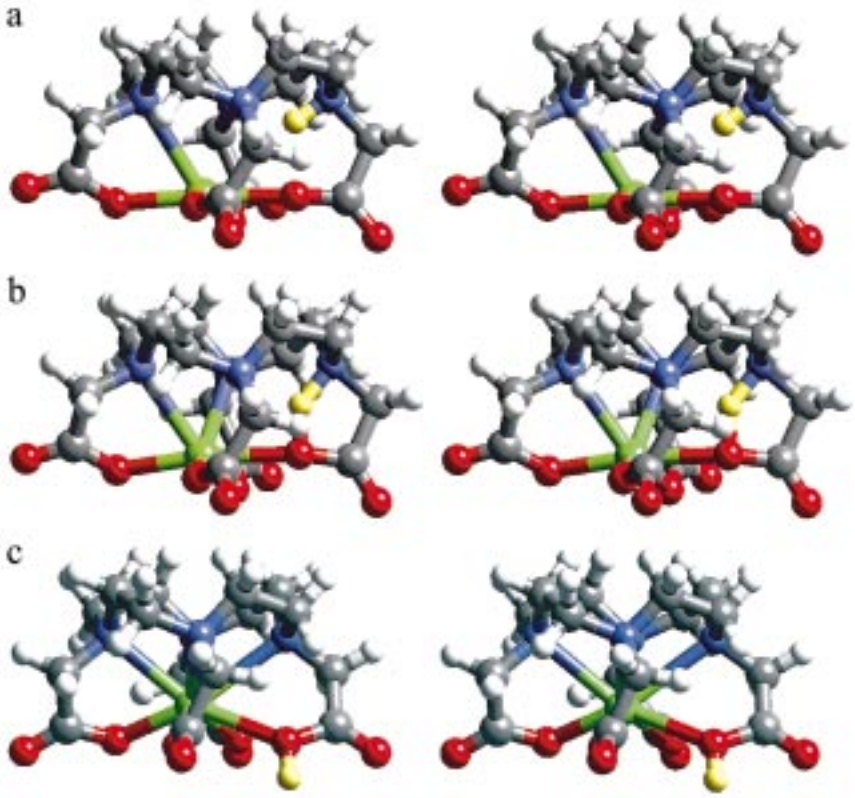

Figure 6. Stereoviews showing proton transfer from the ring nitrogen to the carboxylate oxygen of YH(DOTA); (a) reactant, (b) transition state, and (c) product. The water molecules coordinated in the inner coordination shell are not shown here.

Table 3. Energy and Geometry Changes for Proton Transfer from Ring Nitrogen to Carboxylate Oxygen of YH(DOTA)

		reactant NH···OCO (Figure 6a)	TS N···H···OCO (Figure 6b)	product N···HOCO (Figure 6c)
rel energy (kcal/mol)				
gas phase	HF	0.0	9.2	−29.8
	B3LYP//HF	0.0	2.0	−25.2
aq phase	HF	0.0	20.7	−5.6
	B3LYP//HF	0.0	12.2	−8.8
r(N−H) (Å)		1.016	1.263	3.637
r(O−H) (Å)		1.809	1.180	0.959
r(O−Y) (Å)		2.278	2.201	2.580
		2.176	2.174	2.203
		2.208	2.381	2.225
		2.183	2.178	2.222
r(N−Y) (Å)		3.855	3.868	**2.780**
		2.742	**2.650**	**2.619**
		3.021	**2.758**	**2.654**
		3.357	3.198	**2.724**

Scheme 4. *N*-Dimethylglycine: A Model Representing the Proton Transfer of YH(DOTA)

(a) model reactant (b) model TS

$[(CH_3)_2NH^+CH_2COO^-$; Scheme 4]. We see that the solvation energy of the transition state is 17 kcal/mol lower than that of the reactant. This confirms that desolvation of the transition state due to the charge delocalization can explain the 10-kcal/mol change for YH(DOTA). [The larger desolvation of 17 kcal/mol for the model compound arises because the [N···H···O] part of the model compound is entirely exposed to solvent whereas a part of the [N···H···O] of YH(DOTA) is inside the cage.]

5.2. Rates. Unfortunately, the activation enthalpy for this reaction has not yet been determined experimentally. Instead, the activation free energy $\Delta G^{\ddagger}$ has been estimated from the rate constant k at 25 °C by using the Eyring equation[45] $k = (k_B T/h) \exp[-\Delta G^{\ddagger}/RT]$, where k_B is the Boltzmann constant and h is Planck's constant.[15,17] (This equation was derived for the one-dimensional case (conventional transition state theory) and is approximate for the multidimensional case. Also quantum effects such as tunneling of the proton are not included.) To compare with these experimental rates, we corrected the calculated energy barrier with the change in zero-point energy (ZPE) and thermodynamic functions $[(-TS)_{298K}$ and $\Delta H_{0\rightarrow 298K}]$ obtained from the vibrational analysis (Table 4). This leads to an activation free energy of 8.4 kcal/mol (at 25 °C in aqueous solution at the B3LYP//HF level). This is in good agreement with experimental activation free energies estimated from the rate constants: 8.1, 8.2, and 9.3 kcal/mol for Eu^{3+}, Gd^{3+}, and Ce^{3+} complexes of DOTA.[15,17]

The Hessian used for this vibrational analysis was not from a systematic perturbation of each coordinate of each atom nor from the analytical second derivatives; instead it was the Hessian from updating at each geometry-optimization step. The resultant vibrational frequencies and normal modes, especially the modes that are not involved in the optimization, may not be accurate enough to be used in quantitative estimates of ZPE and thermodynamic functions. Thus, we also considered the proton transfer in the model system $Y-NH(CH_3)_2CH_2COO$. The structures of the reactant and the transition state model are expected to be similar to that of YH(DOTA). For the model we did an accurate analytic vibrational analysis to obtain the ZPE and free-energy corrections. This leads to an activation

(45) Steinfeld, J. I.; Francisco, J. S.; Hase, W. L. *Chemical Kinetics and Dynamics*; Prentice Hall: Englewood Cliffs, NJ, 1989.

Table 4. Activation Free Energy (kcal/mol) of the Proton Transfer from the Ring Nitrogen to the Carboxylate Oxygen of YH(DOTA) in Aqueous Solution

		reactant	TS	barrier
energy barrier (aq)	B3LYP//HF	0	12.2	12.2
zero-point energy	DOTA[a]	300.9	296.8	−4.1
	model[b]	92.9	90.1	−2.6
$(-TS)_{298K}$	DOTA[a]	−43.8	−43.6	0.2
	model[b]	−25.4	−25.5	−0.1
$\Delta H_{0\rightarrow 298K}$	DOTA[a]	14.4	14.6	0.2
	model[b]	5.2	5.6	0.3
activation free energy	DOTA[a]			**8.4**
	model[b]			**9.6**
experiment				8.1 (Eu^{3+})[c]
				8.2 (Gd^{3+})[d]
				9.3 (Ce^{3+})[e]

[a] Vibrational analysis from the approximate Hessian for the whole complex (YH(DOTA)). [b] Vibrational analysis from the analytic Hessian for the model complex ($Y-NH(CH_3)_2CH_2COO$). [c] Reference 15. [d] References 5, 15, and 17. [e] References 5 and 15.

free energy of 9.6 kcal/mol, which is reasonably close to the directly calculated value of 8.4. Thus, these calculations support pathway 3 as the deprotonation pathway for YH(DOTA).

Another set of experimental activation free energy values have been estimated[15] from the same rate constants: 13.7, 13.8, 14.8, and 14.0 kcal/mol for the Eu^{3+}, Gd^{3+}, Ce^{3+}, and Ca^{2+} complexes of DOTA. However, the assumption in deriving these activation energies was that the base-catalyzed deprotonation from the singly protonated intermediate produces an unprotonated activated complex that maintains the coordination of the metal ion only to the carboxylate groups and the rearrangement from this to the final octadentate complex is the rate-determining step. These $\Delta G^{\ddagger}$ values assume that the rearrangement process is separated from the deprotonation. This postulate disagrees with our calculations that show a spontaneous rearrangement following deprotonation.

Thus, we propose the following reaction pathway for formation of $Y(DOTA)^-$: (1) formation of a crab-like 5-coordinate intermediate YH(DOTA) containing a hydrogen bond between N−H and O−C−O; (2) proton transfer from the ring nitrogen to the adjacent carboxylate oxygen, making the proton accessible to outside base (H_2O or OH^- depending on pH); and (3) simultaneous transition of Y^{3+} from outside the cage (5-coordinate) to inside the cage to form a very stable octadentate coordination compound.

6. Suggestion of a New Chelating Agent

On the basis of the mechanism suggested above, we now propose a modification of DOTA expected to accelerate the metal binding by reducing the energy barrier of the rate-determining proton-transfer reaction, $YH(DOTA) \rightarrow Y(DOTA)^- + H^+$. In YH(DOTA), the proton-transfer reaction involves a five-membered ring as a transition state as shown in Figures 6b and 7a. We speculated that the strain caused by the acute angles in this ring and by the nonlinear character of the N···H···O bond might be responsible for the high barrier of this process and the slow formation of the Y−DOTA complex. Thus, we considered the modified DOTA with one additional methylene group ($-CH_2-$) in one of the carboxylate arms of DOTA as shown in Scheme 5. This new chelant [1,4,7,10-tetraazacyclododecane-1,4,7-triacetic acid−10-propionic acid] is denoted as DO3AlPr. We expected the six-membered ring transition state (Figure 7b) to be more stable, leading to a lower energy barrier and faster complex formation.

Scheme 5. Schematic Drawings of (a) DOTA and (b) Newly Suggested DO3A1Pr (1,4,7,10-Tetraaazacyclododecane-1,4,7-triacetic Acid−10-Propionic Acid)[a]

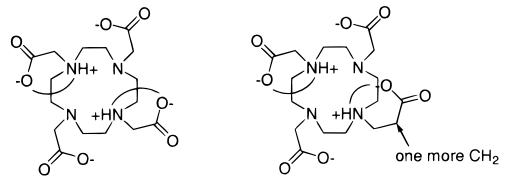

(a) $H_2(DOTA)^{2-}$ (b) $H_2(DO3A1Pr)^{2-}$

[a] These show one of several possible hydrogen-bond-stabilized conformations of free $H_2(DOTA)^{2-}$ and free $H_2(DO3A1Pr)^{2-}$.

Similar arguments have been made in comparing the gas-phase basicities of amino acids.[46] The proton affinity of β-alanine ($NH_3^+CH_2CH_2COO^-$) is 2.6 kcal/mol higher than that of glycine ($NH_3^+CH_2COO^-$), due to the ability of β-alanine to form a stable 6-membered closed ring structure, thereby stabilizing the protonated amine through a strong intramolecular hydrogen bond. Thus, the $N-H^+\cdots O(=C)$ interaction is more linear in β-alanine than in glycine. That is, the structural constraints prohibiting the favorable interaction of the protonated amine with the neighboring carbonyl group in glycine are relaxed with one more methylene unit between these two groups in β-alanine.

To obtain the energy barrier for DO3AlPr, we optimized the geometries of (a) YH(DO3AlPr) with a ring nitrogen protonated and (b) the transition state for proton transfer to its carboxylate [denoted as Y(DO3AlPr)-H].

First, the location of the proton in the macrocycle was determined for YH(DO3A1Pr). We calculated that the protonation is 7.8 kcal/mol more stable (in aqueous solution) on the nitrogen attached to propionate (HNPr; Figure 8a) than on the nitrogen attached to acetate (HNAc; Figure 8b) (see Table 5). This result was expected because the protonation constant (pK_a) of glycine ($NH_3^+CH_2COO^-$) (9.78 at 298.15 K and 9.20 at 323.15 K) is lower than that of β-alanine ($NH_3^+CH_2CH_2COO^-$) (10.238 at 298.15 K and 9.60 at 323.15 K)[47] [i.e., the nitrogen attached to propionate is more basic than the nitrogen attached to acetate]. Moreover, as shown in Figure 8 and Table 5, the $(N-)H\cdots O(CO)$ distance of $HNCH_2CH_2COO^-$ (1.61 Å) is shorter than that of $HNCH_2COO^-$ (1.85 Å) [i.e., the intramolecular hydrogen bond is stronger for HNPr than for HNAc (as discussed earlier for β-alanine and glycine)]. In addition, the $Y^{3+}\cdots H$ distance in HNPr (2.99 Å) is longer than that of HNAc (2.80 Å). Due to the flexibility of the propionate arm in HNPr, Y^{3+} can be located away from the proton to relieve the repulsion between Y^{3+} and the proton more efficiently than in HNAc.

Next we optimized the transition state of the proton-transfer reaction from this nitrogen to propionate oxygen involving the six-membered ring structure. We find (Figure 7 and Table 6) that the transition state of DO3AlPr has less acute angles and a more linear N···H···O bond than for DOTA. As expected, this leads to a significantly lower energy barrier for DO3A1Pr (4.5 kcal/mol as compared to 12.2 kcal/mol for DOTA). We estimate an activation free energy of 3.9 kcal/mol for incorporation of Y^{3+} into the ring of DO3AlPr, which is 4.5 kcal/mol **less** than that for DOTA (8.4 kcal/mol). [Both estimates are based on the Hessian updated during the geometry optimization.] This suggests that incorporation of Y^{3+} may be 2000 times faster

(46) Wu, J.; Gard, E.; Bregar, J.; Green, M. K.; Lebrilla, C. B. *J. Am. Chem. Soc.* **1995**, *117*, 9900−9905.
(47) Gillespie, S. E.; Oscarson, J. L.; Izatt, R. M.; Wang, P.; Renuncio, J. A. R.; Pando, C. *J. Solution Chem.* **1995**, *24*, 1219−1247.

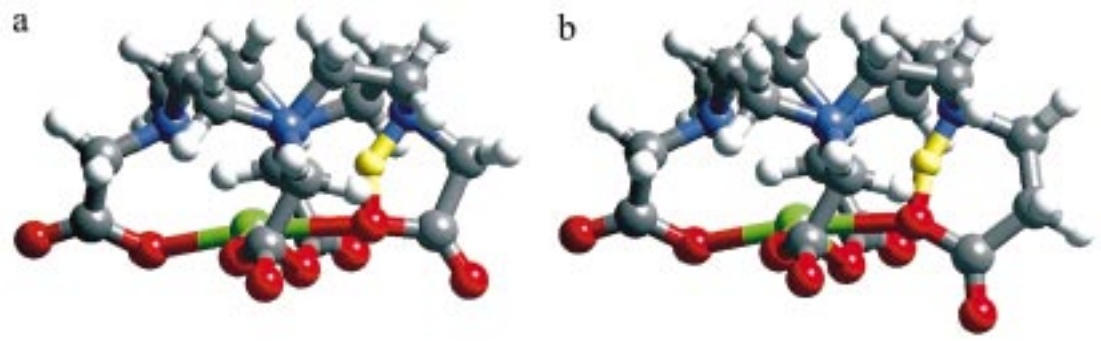

Figure 7. Transition state of the proton transfer from the ring nitrogen to the carboxylate oxygen of (a) YH(DOTA) and (b) newly proposed YH(DO3A1Pr). Note the five-membered ring in YH(DOTA) and the six-membered ring in YH(DO3AlPr). Color key: green, Y; blue, N; red, O; gray, C; white, H; and yellow, H attached to the ring N. The water molecules coordinated in the inner coordination shell are not shown here.

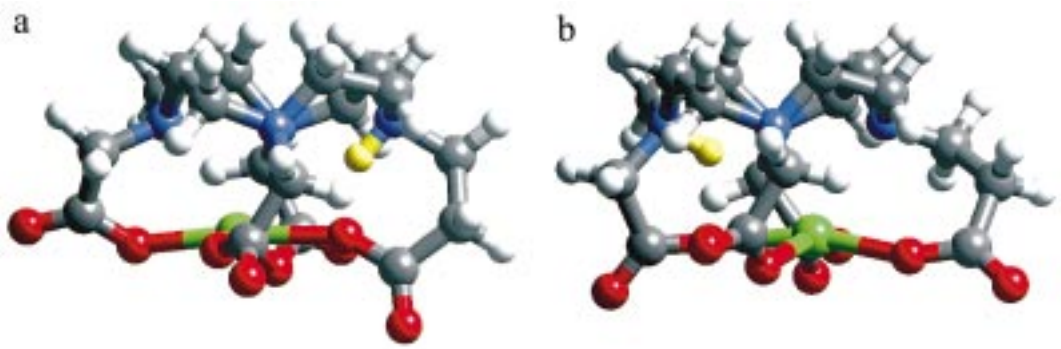

Figure 8. Optimized structures of YH(DO3A1Pr) protonated on two different sites: (a) proton on the nitrogen attached to propionate (HNPr) and (b) proton on the nitrogen attached to acetate (HNAc). Color key: green, Y; blue, N; red, O; gray, C; white, H; and yellow, H attached to the ring N. The water molecules coordinated in the inner coordination shell are not shown here.

Table 5. Energy and Geometry Parameters of Two Isomers of DO3A1Pr

	HNPr (Figure 8a)	HNAc (Figure 8b)
rel energy (kcal/mol)	0.0	7.8
$Y^{3+}\cdots H^{\delta+}$ distance (Å)	2.99	2.80
(N−)H···O(CO) distance (Å)	1.61	1.85

Table 6. Energy Barrier (kcal/mol) and Geometry for the Transition State of Proton Transfer from the Ring Nitrogen to the Carboxylate Oxygen of YH(DOTA) and YH(DO3A1Pr)

transition state		DOTA	DO3A1Pr
energy barrier in	HF	20.7	10.6
the aq phase	B3LYP//HF	12.2	4.5
activation free energy for Type I → II	B3LYP//HF	8.4	3.9
bond length (Å)	*r*(N−H)	1.263	1.236
	r(O−H)	1.180	1.183
angle (deg)	∠O−H−N	143.7	162.3
	∠H−N−C	88.4	95.8
	∠N−C−C	104.5	111.9
	∠C−C−C		114.6
	∠C−C−O	107.6	112.7
	∠C−O−H	95.7	108.8

into DO3A1Pr than into DOTA. Thus, we suggest that DO3A1Pr be tested for radioimmunotherapy using $^{90}Y^{3+}$ and related elements ($^{111}In^{3+}$, Gd^{3+}, etc.).

7. Summary

The structures and energetics of $YH_2(DOTA)^+$, YH(DOTA), and $Y(DOTA)^-$ were calculated with use of ab initio methods. In the doubly protonated intermediate $YH_2(DOTA)^+$, Y^{3+} is coordinated only by four equivalent carboxylate oxygens and is located far away from ring nitrogens. As protons are removed from ring nitrogens, Y^{3+} spontaneously moves toward the ring leading to the final complex $Y(DOTA)^-$ where Y^{3+} is coordinated by all four nitrogens and all four carboxylate oxygens. We find that the YH(DOTA) to $[Y(DOTA)^- + H^+]$ transition is the rate-determining step of the complexation process. We also found that the crab-like 4-coordinate conformation is the most stable conformation of $YH_2(DOTA)^+$ and YH(DOTA). In this conformation, especially for YH(DOTA), the proton that must be removed for complexation is not accessible to solvent, making the complex formation very slow compared with noncyclic analogues such as DTPA.

We then considered the question of how the proton is removed from this YH(DOTA) intermediate. We found that the carboxylate oxygen location (just ∼1.8 Å from the proton attached to the ring nitrogen) is favorable for proton transfer from N to O with an energy barrier of only 12.2 kcal/mol (in aqueous solution). This transfer exposes the proton to outside base. The activation free energy calculated in the aqueous phase is ∼8.4 kcal/mol, in good agreement with experimental results (8.1−9.3 kcal/mol) estimated from the rate constant data for various DOTA complexes.

As the proton is transferred from the ring nitrogen to the carboxylate oxygen, we find that Y^{3+} simultaneously moves toward the ring in a concerted manner to form the final octadentate coordination complex. On the basis of our ab initio calculations, we propose the following reaction pathway for complexation of Y^{3+} by $H(DOTA)^{3-}$: (1) formation of a crab-

like 5-fold coordination intermediate containing a hydrogen bond between N−H and O−C−O [this is the type I species]; (2) proton transfer from the ring nitrogen to its carboxylate oxygen, making the proton more accessible to the outside base (H_2O or OH^- depending on pH) [this is the rate-determining step]; and (3) simultaneous movement of 5-coordinate Y^{3+} to a very stable 8-coordinate site inside the cage [this is the type II species].

On the basis of these results, we designed a modified chelating ligand DO3A1Pr leading to the rate-determining step having a barrier of only 3.9 kcal (cf. 8.4 for DOTA). Thus, we suggest that DO3AlPr be considered as an alternative to DOTA in ^{90}Y radioimmunotherapy.

Acknowledgment. This research was supported by the National Science Foundation (CHE 95-22179, DBI 97-08929, and ASC 92-100368, W.A.G.) and the National Institutes of Health (CA 43904, J.E.S., and HO 36385, W.A.G.). The facilities of the MSC are also supported by DOE-ASCI, ARO-MURI, ARO-DURIP, BP Chemical, Owens-Corning, Exxon Corp., Beckman Institute, Avery-Dennison, Chevron Petroleum Technology Co., Asahi Chemical, Chevron Chemical Company, and Chevron Research and Technology Co. We thank Larry Smarr for access to the NCSA supercomputing facilities.

JA983706Q